G2/C1 Hermite interpolation by planar PH B-spline curves with shape parameter

G^2/C^1 Hermite interpolation by planar PH B-spline curves with shape parameter

Gudrun Albrecht[b], Carolina Vittoria Beccari[a,*], Lucia Romani[a]

[a] *Dipartimento di Matematica, Alma Mater Studiorum Università di Bologna, Italy*
[b] *Escuela de Matemáticas, Universidad Nacional de Colombia, sede Medellín, Colombia*

Abstract

We solve the problem of G^2/C^1 Hermite interpolation (i.e. interpolation of prescribed boundary points as well as first derivatives and curvatures at these points) by planar quintic Pythagorean Hodograph B-spline curves with one free interior knot which acts as a shape parameter. We present conditions on the data ensuring the existence of solutions. Finally, we illustrate the influence of the interior knot on the shape of the resulting interpolant and on the values of the absolute rotation index or the bending energy.

Keywords: Planar B-spline curve; Pythagorean-Hodograph; Hermite interpolation; Shape parameter

1. Introduction

The problem of Hermite interpolation has been of interest to the Pythagorean Hodograph (PH) community since the nineties (see, e.g., [1–7]). In this work we focus on the so called G^2/C^1 Hermite interpolation problem (i.e. interpolation of prescribed boundary points as well as first derivatives and curvatures at these points) since in many applications it is important to interpolate, together with points and curvature values, also first derivatives rather than tangent directions. The main reason is that interpolation of G^2/G^1 boundary data (i.e. points, tangents and curvatures) may lead to poorly parametrized curves. Instead, in several contexts, it is important to approximate not only the original curve, but also its speed distribution along the curve, namely its parameterization.

The G^2/C^1 Hermite interpolation problem has been already successfully solved in [4] using degree-7 polynomials. In our paper we propose a lower degree solution based on quintic PH B-spline curves with one free interior knot whose location influences the shape of the curve. Following the seminal idea used in [8], in the last decade several other authors managed to achieve lower degree PH solutions to various types of Hermite interpolation problems [9–12], where the common denominator is always the construction of PH curves made of two or more pieces. However, to the best of our knowledge, the only existing lower degree solution to the G^2/C^1 Hermite interpolation problem is the one in [5]. In that paper, it is shown the possibility of solving the problem by constructing two PH quintics glued at some point, and it is suggested an empirical strategy to remove the curvature discontinuity at the junction point by manipulating the acceleration components of the boundary conditions. The key improvement of our work consists in automatically guaranteeing the construction of a smooth PH quintic biarc equipped with a shape parameter.

The remainder of this paper is organized as follows. In Section 2 we introduce the G^2/C^1 Hermite interpolation problem and propose an algorithm for computing its solutions by means of planar quintic PH B-spline curves with one free interior knot. In Section 3 we illustrate how to verify the existence of solutions depending on the prescribed initial data. In Section 4 we present some numerical examples and investigate the influence of the interior knot on the shape of the resulting interpolant as well as on the value of its absolute rotation index or bending energy.

*Corresponding author.
Email addresses: galbrecht@unal.edu.co (Gudrun Albrecht), carolina.beccari2@unibo.it (Carolina Vittoria Beccari), lucia.romani@unibo.it (Lucia Romani)

2. The G^2/C^1 Hermite interpolation problem

According to [13, Corollary 1], a C^2-continuous quintic PH B-spline curve

$$\mathbf{r}(t) = \sum_{i=0}^{8} \mathbf{r}_i N_{i,\boldsymbol{\rho}}^5(t)\,, \quad t \in [0,1]\,, \tag{1}$$

defined over the knot vector $\boldsymbol{\rho} = [0,0,0,0,0,0,a,a,a,1,1,1,1,1,1]$ where $a \in (0,1)$ is a free interior knot (see (53) in [13]) is obtained starting from a preimage quadratic spline curve $\mathbf{z}(t) = \sum_{i=0}^{3} \mathbf{z}_i N_{i,\boldsymbol{\mu}}^2(t)$, defined over the partition $\boldsymbol{\mu} = [0,0,0,a,1,1,1]$. The control points of $\mathbf{r}(t)$ depend on a and have the following expressions, where $\mathbf{r}_0$ is arbitrary:

$$\begin{gathered}
\mathbf{r}_1 = \mathbf{r}_0 + \tfrac{a}{5}\,\mathbf{z}_0^2, \qquad \mathbf{r}_2 = \mathbf{r}_1 + \tfrac{a}{5}\,\mathbf{z}_0\mathbf{z}_1, \qquad \mathbf{r}_3 = \mathbf{r}_2 + \tfrac{a}{5}\,\left(\tfrac{2}{3}\mathbf{z}_1^2 + \tfrac{1}{3}\,\mathbf{z}_0\left((1-a)\mathbf{z}_1 + a\mathbf{z}_2\right)\right), \\
\mathbf{r}_4 = \mathbf{r}_3 + \tfrac{\mathbf{z}_1}{5}\,\left((1-a)\mathbf{z}_1 + a\mathbf{z}_2\right), \qquad \mathbf{r}_5 = \mathbf{r}_4 + \tfrac{\mathbf{z}_2}{5}\,\left((1-a)\mathbf{z}_1 + a\mathbf{z}_2\right), \\
\mathbf{r}_6 = \mathbf{r}_5 + \tfrac{(1-a)}{5}\,\left(\tfrac{2}{3}\mathbf{z}_2^2 + \tfrac{1}{3}\,\mathbf{z}_3\left((1-a)\mathbf{z}_1 + a\mathbf{z}_2\right)\right), \qquad \mathbf{r}_7 = \mathbf{r}_6 + \tfrac{1-a}{5}\,\mathbf{z}_2\mathbf{z}_3, \qquad \mathbf{r}_8 = \mathbf{r}_7 + \tfrac{1-a}{5}\,\mathbf{z}_3^2\,.
\end{gathered} \tag{2}$$

We will now use these curves in order to solve the following G^2/C^1 Hermite interpolation problem: Given arbitrary boundary points $\mathbf{p}_0$, $\mathbf{p}_1$, first derivatives $\mathbf{d}_0$, $\mathbf{d}_1$ at the boundary and corresponding curvature values κ_0, κ_1, we look for the control points $\mathbf{r}_0, \mathbf{r}_1, \ldots, \mathbf{r}_8$ of the PH quintic B-spline curve (1) such that $\mathbf{r}(0) = \mathbf{p}_0\,,\ \mathbf{r}(1) = \mathbf{p}_1\,,\ \mathbf{r}'(0) = \mathbf{d}_0\,,\ \mathbf{r}'(1) = \mathbf{d}_1\,,\ \kappa(0) = \kappa_0\,,\ \kappa(1) = \kappa_1$.

According to (2) this means that we have to determine the control points $\mathbf{z}_i := u_i + \mathbf{i}\,v_i$, $i = 0,\ldots,3$, of the preimage curve $\mathbf{z}(t)$. The positional interpolation constraints clearly imply $\mathbf{r}_0 = \mathbf{p}_0$ and $\mathbf{r}_8 = \mathbf{p}_1$. In addition, the first derivative interpolation constraints yield the following conditions:

$$\begin{aligned}
\mathbf{r}'(0) = \mathbf{z}^2(0) = \mathbf{z}_0^2 = \mathbf{d}_0 = d_0(\cos(\omega_0) + \mathbf{i}\,\sin(\omega_0))\,, \quad d_0 \geq 0\,, \\
\mathbf{r}'(1) = \mathbf{z}^2(1) = \mathbf{z}_3^2 = \mathbf{d}_1 = d_1(\cos(\omega_1) + \mathbf{i}\,\sin(\omega_1))\,, \quad d_1 \geq 0\,.
\end{aligned} \tag{3}$$

By applying de Moivre's theorem to the two equations in (3) we obtain the following solutions for $\mathbf{z}_0$ and $\mathbf{z}_3$, where $\omega_l = \arg(\mathbf{d}_l) \in [0, 2\pi)$ for $l = 0, 1$:

$$\begin{aligned}
\mathbf{z}_0 = u_0 + \mathbf{i}\,v_0 = (-1)^k\sqrt{d_0}\left(\cos\left(\frac{\omega_0}{2}\right) + \mathbf{i}\,\sin\left(\frac{\omega_0}{2}\right)\right),\ k \in \{0,1\}\,, \\
\mathbf{z}_3 = u_3 + \mathbf{i}\,v_3 = (-1)^j\sqrt{d_1}\left(\cos\left(\frac{\omega_1}{2}\right) + \mathbf{i}\,\sin\left(\frac{\omega_1}{2}\right)\right),\ j \in \{0,1\}.
\end{aligned} \tag{4}$$

Note that we can limit ourselves to considering the combinations of $\mathbf{z}_0$, $\mathbf{z}_3$ with signs $+,+$ and $+,-$, i.e., $k = j = 0$ and $k = 0$, $j = 1$, since the others will give rise to the same solutions. Next, recalling the general formula for the curvature of a PH curve (see, e.g., [6]) $\kappa(t) = 2\,(\mathrm{Im}\Big(\overline{\mathbf{z}}(t)\,\mathbf{z}'(t)\Big))/(|\mathbf{z}(t)|^4)$, we can express the curvature constraints at $t = 0$ and $t = 1$ as

$$\kappa(0) = \frac{4}{a}\cdot\frac{\mathrm{Im}(\bar{\mathbf{z}}_0\mathbf{z}_1)}{|\mathbf{z}_0|^4} = \frac{4}{a}\cdot\frac{u_0v_1 - u_1v_0}{(u_0^2+v_0^2)^2} = \kappa_0\,, \qquad \kappa(1) = \frac{4}{1-a}\cdot\frac{\mathrm{Im}(\bar{\mathbf{z}}_3\mathbf{z}_2)}{|\mathbf{z}_3|^4} = \frac{4}{1-a}\cdot\frac{u_2v_3 - u_3v_2}{(u_3^2+v_3^2)^2} = \kappa_1\,. \tag{5}$$

If $u_0 \neq 0$, i.e., $\omega_0 \neq \pi$, and $u_3 \neq 0$, i.e., $\omega_1 \neq \pi$, we can derive v_1 and v_2 from (5), obtaining

$$v_1 = \frac{1}{u_0}\left(u_1v_0 + \frac{a}{4}\kappa_0(u_0^2+v_0^2)^2\right), \qquad v_2 = \frac{1}{u_3}\left(u_2v_3 - \frac{(1-a)}{4}\kappa_1(u_3^2+v_3^2)^2\right). \tag{6}$$

If $u_0 = 0$, respectively, $u_3 = 0$, i.e., if $\omega_0 = \pi$, respectively, $\omega_1 = \pi$, we can not proceed as in (6), therefore we always assume not to be in this situation.

To determine the remaining unknowns u_1 and u_2 in (6) we consider the equation

$$\mathbf{r}_7 - \mathbf{r}_1 = \sum_{i=1}^{6}\Delta\mathbf{r}_i\,, \quad \text{with} \quad \Delta\mathbf{r}_i = \mathbf{r}_{i+1} - \mathbf{r}_i. \tag{7}$$

Since $\mathbf{r}'(0) = \frac{5}{a}(\mathbf{r}_1 - \mathbf{r}_0) = \mathbf{d}_0\,,\ \ \mathbf{r}'(1) = \frac{5}{1-a}(\mathbf{r}_8 - \mathbf{r}_7) = \mathbf{d}_1$ the left hand side of equation (7) is completely determined by the given Hermite data as:

$$\mathbf{r}_7 - \mathbf{r}_1 = \mathbf{r}_8 - \mathbf{r}_0 - \frac{(1-a)}{5}\,\mathbf{d}_1 - \frac{a}{5}\,\mathbf{d}_0 = \mathbf{p}_1 - \mathbf{p}_0 - \frac{(1-a)}{5}\,\mathbf{d}_1 - \frac{a}{5}\,\mathbf{d}_0.$$

By (2) the right hand side of (7) reads as

$$\frac{1}{5}(1-\frac{a}{3})\mathbf{z}_1^2 + \frac{1}{15}(2+a)\mathbf{z}_2^2 + \frac{1}{5}\mathbf{z}_1\mathbf{z}_2 + \frac{1}{15}(1-a)^2\mathbf{z}_1\mathbf{z}_3 + \frac{1}{15}a(4-a)\mathbf{z}_0\mathbf{z}_1 + \frac{1}{15}(3-2a-a^2)\mathbf{z}_2\mathbf{z}_3 + \frac{1}{15}a^2\mathbf{z}_0\mathbf{z}_2. \quad (8)$$

By separating the real and imaginary parts of the last equation we obtain a system of two real quadratic equations in the two real unknowns u_1 and u_2 having the form:

$$C_A\ :\ \ \mathbf{u}^T A\mathbf{u} = 0\,, \qquad C_B\ :\ \ \mathbf{u}^T B\mathbf{u} = 0\,, \quad (9)$$

with $\mathbf{u} = (1, u_1, u_2)^T$ and 3×3 real symmetric matrices $A = (a_{i,j})_{0\le i,j\le 2}$ and $B = (b_{i,j})_{0\le i,j\le 2}$, whose coefficients depend on the given geometric data and can be easily determined by symbolic computations. The two equations in (9) represent conic sections in the real Euclidean plane. Whenever these conics are real and have real intersection points, finding the solutions u_1, u_2 of these equations is equivalent to determining the intersection points of the two conic sections. In order to obtain the intersection points we consider the pencil of conic sections defined by the conics C_A and C_B as

$$\mathbf{u}^T(A + \lambda B)\mathbf{u} = 0\,, \ \ \lambda \in \mathbb{R}. \quad (10)$$

Among the one–parameter set of conics there are between one and three degenerate conics (see e.g., [14]) given by the λ-values obtained as solutions of the cubic equation in λ:

$$\det(A+\lambda B) = \lambda^3 \det(B) + \lambda^2(\det(B_3)+\det(B_2)+\det(B_1)) + \lambda(\det(A_3)+\det(A_2)+\det(A_1)) + \det(A) = 0\,, \quad (11)$$

where the matrices A_k for $k = 1, 2, 3$ are obtained by replacing the k-th column of A by the k-th column of B, and the matrices B_k for $k = 1, 2, 3$ are obtained by replacing the k-th column of B by the k-th column of A. These degenerate conics can be either pairs of distinct real, conjugate complex, or coinciding lines. The intersection points of the conics of the pencil (10) are then easily obtained in the following way. For a solution of the cubic equation (11), by inserting the corresponding λ-value into the equation (10) a quadratic equation easily decomposable into two linear factors is obtained. These two linear equations in u_1 and u_2 can be solved for, e.g., u_1 in dependency of u_2, which are then inserted into another conic of the pencil, for example one of the given conics or another degenerate one, yielding a quadratic equation in u_2. This procedure yields the coordinates of the intersection points of the pencil conics, whenever they exist. The control points of the corresponding PH B-spline curves are obtained by inserting the obtained u_i, v_i, $i = 0, \ldots, 3$ into the expression for $\mathbf{r}_i$ in (2).

The total number of solutions of our interpolation problem is hence $\delta = \delta^{++} + \delta^{+-}$, where δ^{++} respectively δ^{+-}, are the number of real intersection points of the conics from (9) for the sign choice $++$ respectively $+-$ in (4). Among all solutions, the user is usually interested in the interpolating curve with minimum absolute rotation index and bending energy (see, e.g., [1, 15]). The selected examples, included in the following, show interpolation problems with $\delta = 4$ (see Fig. 2) and $\delta = 8$ (see Fig. 3) solutions, respectively.

3. Existence of solutions

In the following we study the existence of a solution for the G^2/C^1 Hermite interpolation problem. Assigned a set of points, first derivatives and curvatures, there are two situations where a solution may not be found. The first corresponds to the case where either A or B (or both) in (9) yield imaginary conics. The second is the case where the two conics in (9) are real, but have no intersection.

Regarding the first problematic case, for a generic conic $C_M:\ \ m_{1,1}u_1^2 + 2m_{1,2}u_1u_2 + m_{2,2}u_2^2 + 2m_{0,1}u_1 + 2m_{0,2}u_2 + m_{0,0} = 0$ with symmetric matrix $M := (m_{i,j})_{0\le i,j\le 2}, m_{i,j} = m_{j,i}$, we suppose $m_{0,0} \ge 0$ and we

denote by $\widetilde{M} := (m_{i,j})_{1\le i,j\le 2}$ the 2×2 matrix of the associated quadratic form. We then consider the following invariants: $I_1^{[M]} := \mathrm{trace}(\widetilde{M})$, $I_2^{[M]} := \det(\widetilde{M})$, $I_3^{[M]} := \det(M)$.

It is useful to observe that, for $M \in \{A, B\}$, $I_1^{[M]}$ and $I_2^{[M]}$ only depend on the knot a and on the angles ω_0, ω_1 defined by the input first derivatives. Here, $I_1^{[M]}$ is linear in a whereas $I_2^{[M]}$ quadratic in a. Instead $I_3^{[M]}$ depend on a, d_0, d_1, ω_0, ω_1, κ_0, κ_1 and are quintic polynomials in a and quadratic in κ_0, κ_1. For $I_2^{[M]} < 0$ the conic is either a hyperbola or a pair of intersecting lines, i.e., real conics extending to infinity. Thus both conics C_A and C_B are real if $I_2^{[A]} < 0$ and $I_2^{[B]} < 0$. In particular, we obtain

$$\begin{aligned} I_2^{[A]} &= \frac{-(\cos(\omega_0)\cos(\omega_1)(4(a-\frac{1}{2})^2-25)+9\cos(\frac{(\omega_0+\omega_1)}{2})^2)}{900\cos(\frac{\omega_0}{2})^2\cos(\frac{\omega_1}{2})^2}, \\ I_2^{[B]} &= \frac{-(4\tan(\frac{\omega_0}{2})\tan(\frac{\omega_1}{2})\cos(\frac{\omega_0}{2})^2\cos(\frac{\omega_1}{2})^2(4(a-\frac{1}{2})^2-25)+9\sin(\frac{(\omega_0+\omega_1)}{2})^2)}{900\cos(\frac{\omega_0}{2})^2\cos(\frac{\omega_1}{2})^2}, \end{aligned}$$

from which one can see that

$$I_2^{[A]} < 0 \;\Leftrightarrow\; \begin{cases} f(\omega_0,\omega_1) := \frac{\cos(\omega_0)\cos(\omega_1)}{\cos(\frac{\omega_0+\omega_1}{2})^2} < -\frac{9}{4(a-\frac{1}{2})^2-25} \;\text{ for }\; \omega_0+\omega_1 \neq \pi \;\text{ and }\; \omega_0+\omega_1 \neq 3\pi, \\ -\cos(\omega_0)^2 < 0 \;\text{ for }\; \omega_0+\omega_1 = \pi \;\text{ or }\; \omega_0+\omega_1 = 3\pi, \end{cases} \tag{14}$$

and

$$I_2^{[B]} < 0 \;\Leftrightarrow\; \begin{cases} g(\omega_0,\omega_1) := \frac{4\tan(\frac{\omega_0}{2})\tan(\frac{\omega_1}{2})\cos(\frac{\omega_0}{2})^2\cos(\frac{\omega_1}{2})^2}{\sin(\frac{\omega_0+\omega_1}{2})^2} < -\frac{9}{4(a-\frac{1}{2})^2-25} \;\text{ for }\; \omega_0+\omega_1 \neq 0 \;\text{ and }\; \omega_0+\omega_1 \neq 2\pi, \\ \tan\left(\frac{\omega_0}{2}\right)^2\cos\left(\frac{\omega_0}{2}\right)^4 > 0 \;\text{ for }\; \omega_0+\omega_1 = 0 \;\text{ or }\; \omega_0+\omega_1 = 2\pi. \end{cases} \tag{15}$$

The second line of (14) is equivalent to $I_2^{[A]} < 0 \Leftrightarrow \omega_0+\omega_1 = \pi$ or $\omega_0+\omega_1 = 3\pi$, where $\omega_0 \notin \{\frac{\pi}{2}, \frac{3}{2}\pi\}$, whereas the second line of (15) to $I_2^{[B]} < 0 \Leftrightarrow \omega_0+\omega_1 = 2\pi$, where $\omega_0 \notin \{0, \pi\}$. Using the fact that $a \in (0,1)$, after some computations one finds that $I_2^{[A]} < 0$ and $I_2^{[B]} < 0$ in either one of the following cases:

1. $f(\omega_0,\omega_1) < \frac{9}{25}$ and $g(\omega_0,\omega_1) < \frac{9}{25}$ for $\omega_0+\omega_1 \notin \{k\pi\}$ for $k = 0,1,2,3$;
2. $\omega_0+\omega_1 = \pi$ or $\omega_0+\omega_1 = 3\pi$ where $\omega_0 \notin \{\frac{\pi}{2}, \frac{3\pi}{2}\}$ and $g(\omega_0,\omega_1) < \frac{9}{25}$;
3. $\omega_0+\omega_1 = 2\pi$ where $\omega_0 \notin \{0,\pi\}$ and $f(\omega_0,\omega_1) < \frac{9}{25}$.

The above conditions 1., 2., 3. translate into constraints on the choices of the directions of first derivatives, that is on the angles ω_0 and ω_1. Figure 1 illustrates the ranges for the angles ω_0 and ω_1 satisfying the inequalities at item 1. By comparing the symbolic expressions of A and B, it is easily seen that the two conics can be coincident only if $\omega_0 = \omega_1 = \pi/4 + k\pi$, $k \in \{0,1\}$. The stated conditions exclude the case $\omega_0 = \omega_1$, thus guaranteeing that the two real conics are distinct. A further analysis also shows that these conditions are always satisfied whenever the angle between $\mathbf{d}_0$ and $\mathbf{d}_1$ is greater than $3/5\pi$ (see Fig. 1 bottom).

The second problematic situation, where the two conics are real, but have no real intersection points, i.e. have four imaginary intersection points, has been characterized in [16] by considering the nature of the degenerate conics in (10). In order to state the conditions we need the abbreviations $\Delta_M := \det(M)$ and $\theta_M := \sum_{i=1}^{3}\det(M_i)$, for $M \in \{A, B\}$, as well as $\Sigma_M := M_{00}u^2 + M_{11}v^2 + M_{22}w^2 + M_{12}2vw + M_{02}2uw + M_{01}2uv$, where M_{ij} is the (i,j)-th cofactor of the matrix M, and u, v, w are arbitrary real variables standing for line coordinates in the projective plane. Furthermore we need $\phi = C_{00}u^2 + C_{11}v^2 + C_{22}w^2 + C_{12}2vw + C_{02}2uw + C_{01}2uv$, where

$$\begin{aligned} &C_{00} = b_{11}a_{22} + a_{11}b_{22} - 2a_{12}b_{12}, \quad C_{01} = b_{12}a_{02} + a_{12}b_{02} - b_{22}a_{01} - a_{22}b_{01}, \quad C_{02} = b_{12}a_{01} + a_{12}b_{01} - b_{11}a_{02} - a_{11}b_{02}, \\ &C_{11} = b_{00}a_{22} + a_{00}b_{22} - 2a_{02}b_{02}, \quad C_{12} = b_{02}a_{01} + a_{02}b_{01} - b_{00}a_{12} - a_{00}b_{12}, \quad C_{22} = b_{00}a_{11} + a_{00}b_{11} - 2a_{01}b_{01}, \end{aligned}$$

as well as

$$p = \frac{\Sigma_B(-\theta_B^2+2\theta_A\Delta_B)-3\Delta_B^2\Sigma_A+\theta_B\Delta_B\phi}{\Delta_B^2},$$
$$q = \frac{\Sigma_B^2(\theta_A^2-2\theta_B\Delta_A)+3\Sigma_A^2\Delta_B^2+\Sigma_A\Sigma_B(2\theta_B^2-4\theta_A\Delta_B)+\Sigma_B\phi(3\Delta_A\Delta_B-\theta_A\theta_B)-2\Sigma_A\phi\Delta_B\theta_B+\phi^2\theta_A\Delta_B}{\Delta_B^2}.$$

According to [16], the two conics C_A and C_B have four imaginary intersection points, i.e., our interpolation problem does not have a solution, if and only if

$$D > 0 \quad \text{and} \quad \sqrt{p^2-3q} - p > 0 \quad \text{for all values of } u, v, w \tag{16}$$

where $D := \theta_A^2\theta_B^2 + 18\Delta_A\Delta_B\theta_A\theta_B - 27\Delta_A^2\Delta_B^2 - 4\Delta_A\theta_B^3 - 4\Delta_B\theta_A^3$ is the pencil's discriminant. Unfortunately, these inequalities formally expressed in terms of our data are highly cumbersome, even if we choose special values for (u, v, w), such as, e.g., $(1, 0, 0)$. Therefore we propose to use this condition in order to check numerically whether or not it holds for the chosen data.

4. Numerical examples and role of the interior knot

We consider first derivative vectors which fulfill the conditions illustrated in Fig. 1. Then, the input curvature values are either sampled from the cubic polynomial interpolating the prescribed points and derivatives (as in Fig. 2) or arbitrarily selected by the user (as in Fig. 3).

The algorithm to be followed for computing all the solutions to the G^2/C^1 Hermite interpolation problem reads as follows. Derive the values of $\mathbf{z}_0$ and $\mathbf{z}_3$ (namely u_0, v_0, u_3, v_3) from (4). Hence, substitute in (8) any combination of $\mathbf{z}_0$ and $\mathbf{z}_3$ to be considered (i.e. taking signs $+,+$ and $+,-$ in (4)), along with the resulting values of v_1 and v_2 given by (6), and derive the two conics C_A and C_B in (9). Check the inequalities in (16) and, if it turns out that C_A and C_B have real intersection points, compute them. Each intersection point will give rise to a solution for u_1, u_2 that identifies a different PH B-spline interpolant that matches the given Hermite boundary data.

In Figures 2 and 3 we display the conics C_A and C_B in the first column, whereas in all other columns we show the PH B-spline curves corresponding to all the intersection points between the two conics. Although the conics for the sign choice $++$ and $+-$ are very similar, they originate very different Hermite interpolants. Among all, the ones with minimum absolute rotation index and bending energy can be easily identified.

Figure 4 shows the shape effects inherited by the PH B-spline interpolant when the interior knot is modified. The first two subfigures from left illustrate the shape modifications achieved by the two interpolants from Figure 3 with smaller values of absolute rotation index (Rabs) and bending energy (Bend). The rightmost subfigure is instead obtained by interpolating a set of symmetric data, consisting of points $\mathbf{p}_0 = (0, 0)$, $\mathbf{p}_1 = (1, 0)$ and derivatives $\mathbf{d}_0 = (-1.5965, 2.7297)$, $\mathbf{d}_1 = (-1.5965, -2.7297)$ such that $\omega_1 = -\omega_0 + 2\pi$. The input value of κ_0 and κ_1 is -0.569210, which is computed by evaluating at each endpoint the curvature of the cubic polynomial interpolating the prescribed points and derivatives. The displayed results show that, for $a = 0.5$, the symmetry in the data is preserved whereas, for the two other choices of a, the curve is attracted towards the first or last edge of the control polygon, respectively, in the same way as it happens with B-spline curves.

In Figure 5 we illustrate different benefits provided by the interior knot. In particular we use the value of a to minimize the absolute rotation index or the bending energy for the input data considered in Figure 4.

5. Conclusions and future research directions

We have introduced a method to interpolate G^2/C^1 Hermite boundary data by planar quintic PH B-spline curves that benefit from a free interior knot. This knot is shown to provide the user with a tool that can be used either to modify the shape of the interpolant or to achieve lower values of the bending energy and absolute rotation index. Directions for further study include the extension of the proposed Hermite interpolation method to spatial quintic PH B-spline curves with one free interior knot and to Minkowski PH (MPH) curves.

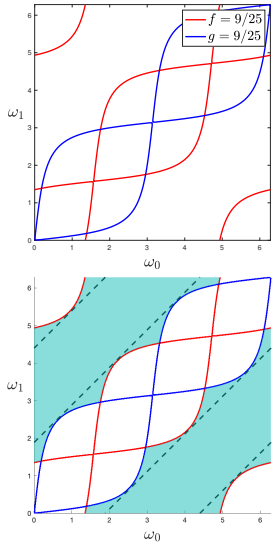

Figure 1: Top: The borders of the two regions where $I_2^{[A]} < 0$ (red) and $I_2^{[B]} < 0$ (blue). Bottom: The two regions in which $\mathbf{d}_0$ and $\mathbf{d}_1$ form an angle greater than $3/5\pi$, the dashed lines corresponding to $3/5\pi$. (For interpretation of the references to color in this figure legend, the reader is referred to the web version of this article.)

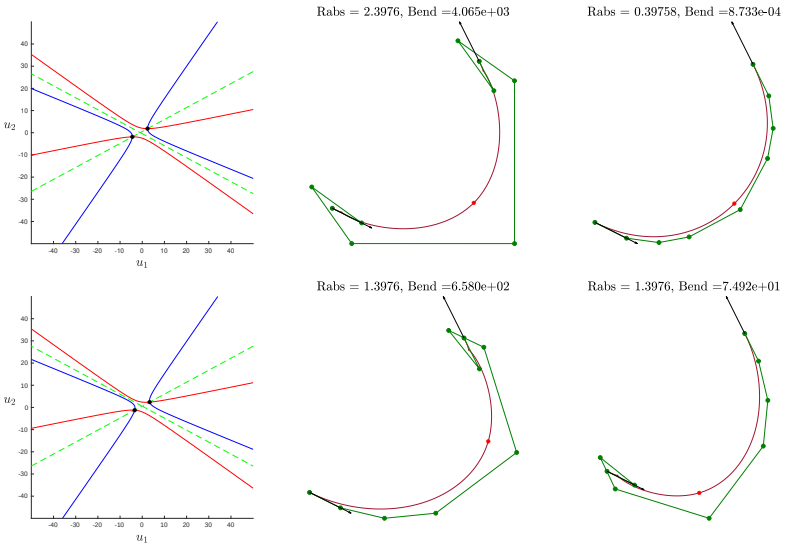

Figure 2: Input data $\mathbf{p}_0 = (1, 0)$, $\mathbf{p}_1 = (4, 3)$, $\mathbf{d}_0 = (6, -3)$, $\mathbf{d}_1 = (-3, 6)$, $\kappa_0 = \kappa_1 = 0.3578$ (where the latter are taken from the cubic polynomial interpolating $\mathbf{p}_0$, $\mathbf{p}_1$, $\mathbf{d}_0$, $\mathbf{d}_1$) and solutions of the case ++ (top) +− (bottom). Left: The two conics C_A (blue) and C_B (red) and a degenerate conic (dashed green). Center and right: The PH B-spline curves corresponding to the two intersection points of the conics and their control polygon. The arrows represent the normalized first derivatives and the red bullet is the image of $a = 0.5$. (For interpretation of the references to color in this figure legend, the reader is referred to the web version of this article.)

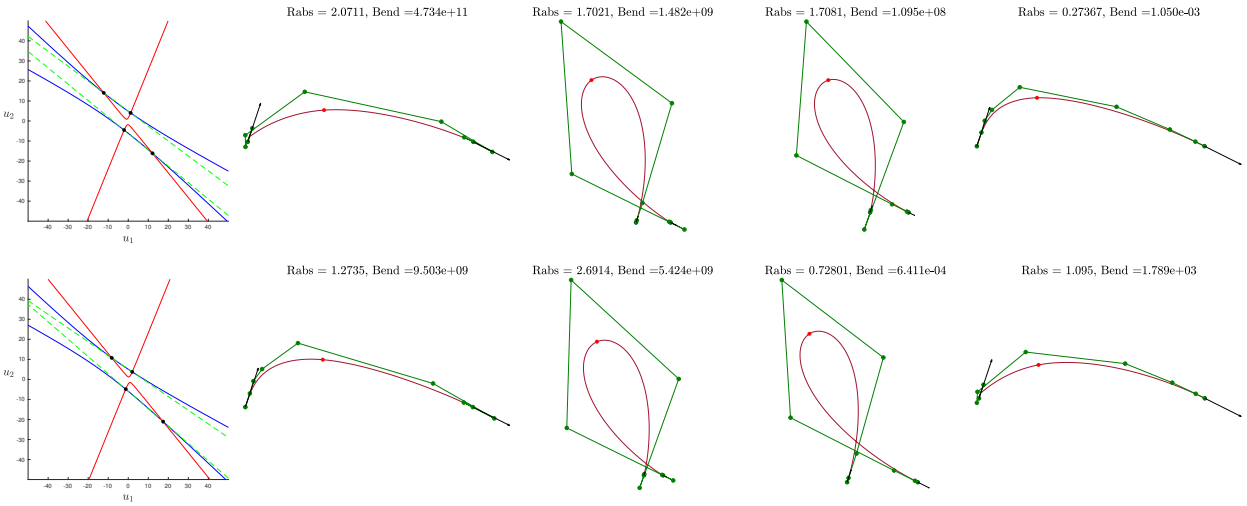

Figure 3: Input data $\mathbf{p}_0 = (0, 0)$, $\mathbf{p}_1 = (5, 0)$, $\mathbf{d}_0 = (1, 3)$, $\mathbf{d}_1 = (2, -1)$, $\kappa_0 = 0.1$, $\kappa_1 = -0.2$ (taken from [5, Example 5]) and solutions of the case ++ (top) +− (bottom). Leftmost column: The two conics C_A (blue) and C_B (red) and a degenerate conic (dashed green). Other columns: The PH B-spline curves corresponding to the four intersection points of the conics and their control polygon. The arrows represent the normalized first derivatives and the red bullet is the image of $a = 0.5$. (For interpretation of the references to color in this figure legend, the reader is referred to the web version of this article.)

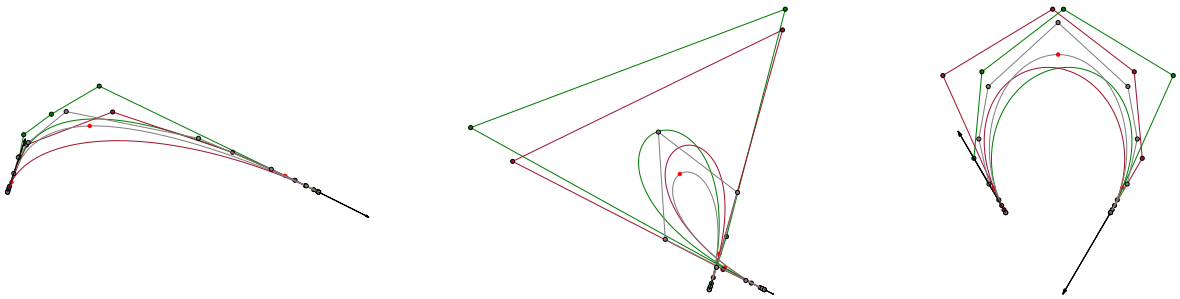

Figure 4: Comparison of curves obtained with interior knot $a = 0.05$, $a = 0.5$ and $a = 0.95$ used as shape parameter.

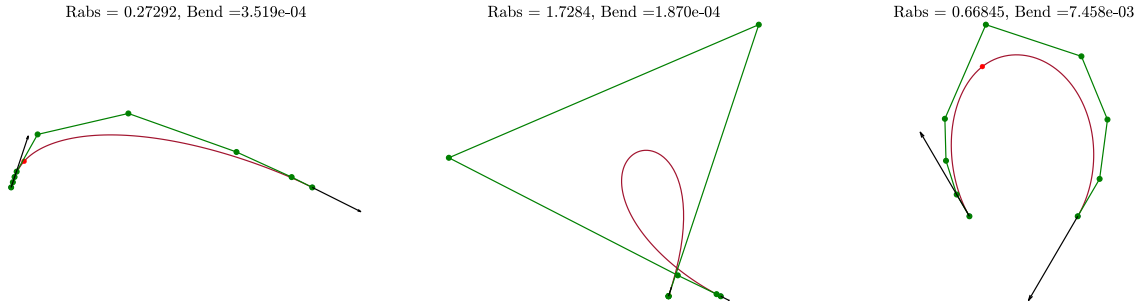

Figure 5: Curves obtained by setting a to minimize the absolute rotation index (Rabs) or the bending energy (Bend) for the data in Fig. 4. From left to right: $a = 0.1435$ corresponding to the minimum Rabs; $a = 1.0e-03$ corresponding to the minimum Bend; $a = 0.3676$ corresponding to the minimum Bend. Note that for the rightmost dataset the minimum Rabs (≈ 0.66845) is obtained for $a = 0.5$ and the corresponding curve is shown in Fig. 4 right.

Acknowledgements

The second and third author are members of INdAM - GNCS, which partially supported this work.

References

[1] R. Farouki, C. Neff, Hermite interpolation by Pythagorean hodograph quintics, Math. Comp. 64 (1995) 1589–1609.
[2] G. Jaklic, J. Kozak, M. Krajnc, V. Vitrih, E. Zagar, On interpolation by planar cubic G^2 Pythagorean-hodograph spline curves, Mathematics of Computation 79 (2010) 305–326.
[3] G. Jaklic, J. Kozak, M. Krajnc, V. Vitrih, E. Zagar, Interpolation by G^2 quintic Pythagorean-hodograph curves, Numerical Mathematics: Theory, Methods and Applications 7 (2014) 374–398.
[4] B. Jüttler, Hermite interpolation by Pythagorean hodograph curves of degree seven, Mathematics of Computation 70 (2001) 1089–1111.
[5] J. Kong, S. Jeong, G. Kim, Hermite interpolation using PH curves with undetermined junction points, Bull. Korean Math. Soc. 49 (2012) 175–195.
[6] L. Romani, L. Saini, G. Albrecht, Algebraic-Trigonometric Pythagorean-Hodograph curves and their use for Hermite interpolation, Advances in Computational Mathematics 40 (2014) 977–1010.
[7] D. Walton, D. Meek, G^2 curve design with a pair of Pythagorean Hodograph quintic spiral segments, Computer Aided Geometric Design 24 (2007) 267–285.
[8] R. Farouki, J. Peters, Smooth curve design with double-Tschirnhausen cubics, Ann. Numerical Math. 3 (1996) 63–82.
[9] B. Bastl, K. Slaba, M. Byrtus, Planar C^1 Hermite interpolation with uniform and non-uniform TC-biarcs, Computer Aided Geometric Design 30 (2013) 58 – 77.
[10] B. Bastl, M. Bizzarri, K. Ferjancic, B. Kovac, M. Krajnc, M. Lavicka, K. Michalkova, Z. Šír, E. Zagar, C^2 Hermite interpolation by Pythagorean-Hodograph quintic triarcs, Computer Aided Geometric Design 31 (2014) 412 – 426.
[11] B. Bastl, M. Bizzarri, M. Krajnc, M. Lavicka, K. Slaba, Z. Šír, V. Vitrih, E. Zagar, C^1 Hermite interpolation with spatial Pythagorean-Hodograph cubic biarcs, Journal of Computational and Applied Mathematics 257 (2014) 65–78.
[12] M. Bizzarri, M. Lavicka, J. Vrsek, C^d Hermite interpolations with spatial Pythagorean hodograph B-splines, Computer Aided Geometric Design 87 (2021) 101992.

[13] G. Albrecht, C. V. Beccari, J.-C. Canonne, L. Romani, Planar Pythagorean-Hodograph B-Spline curves, Computer Aided Geometric Design 57 (2017) 57 – 77.
[14] U. Persson, Pencil of conics, Normat 60 (2012) 1–3.
[15] R. Farouki, The elastic bending energy of Pythagorean-hodograph curves, Computer Aided Geometric Design 13 (1996) 227–241.
[16] J. Johnston, The intersection of two conic sections, Proceedings of the London Mathematical Society s2-3 (1905) 390–402.